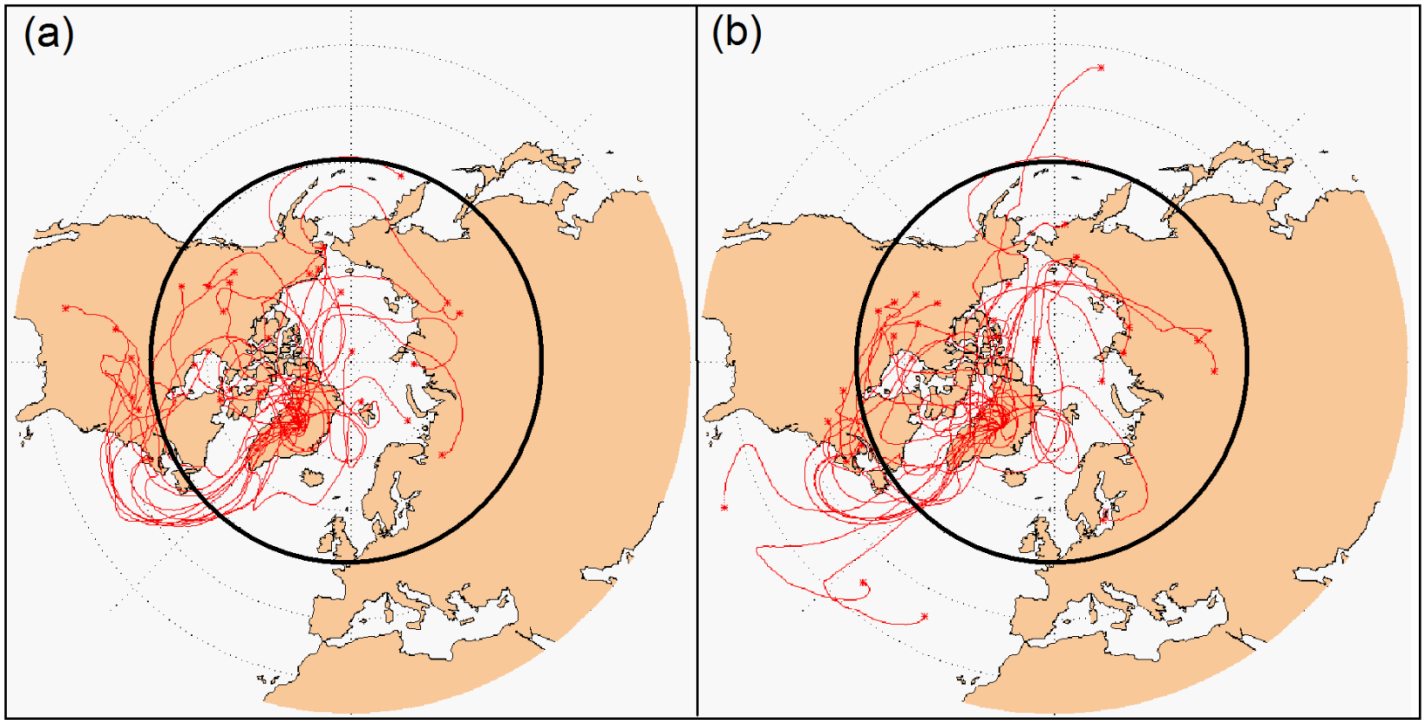

Figure S1. Daily back trajectories starting at 600 hPa above Summit Station for 00z (a) and 12Z (b) during July 2012. End points are indicated by the "*". The 50^{o}N latitude rings are shown revealing the majority of the trajectories originating in the more northern latitudes.

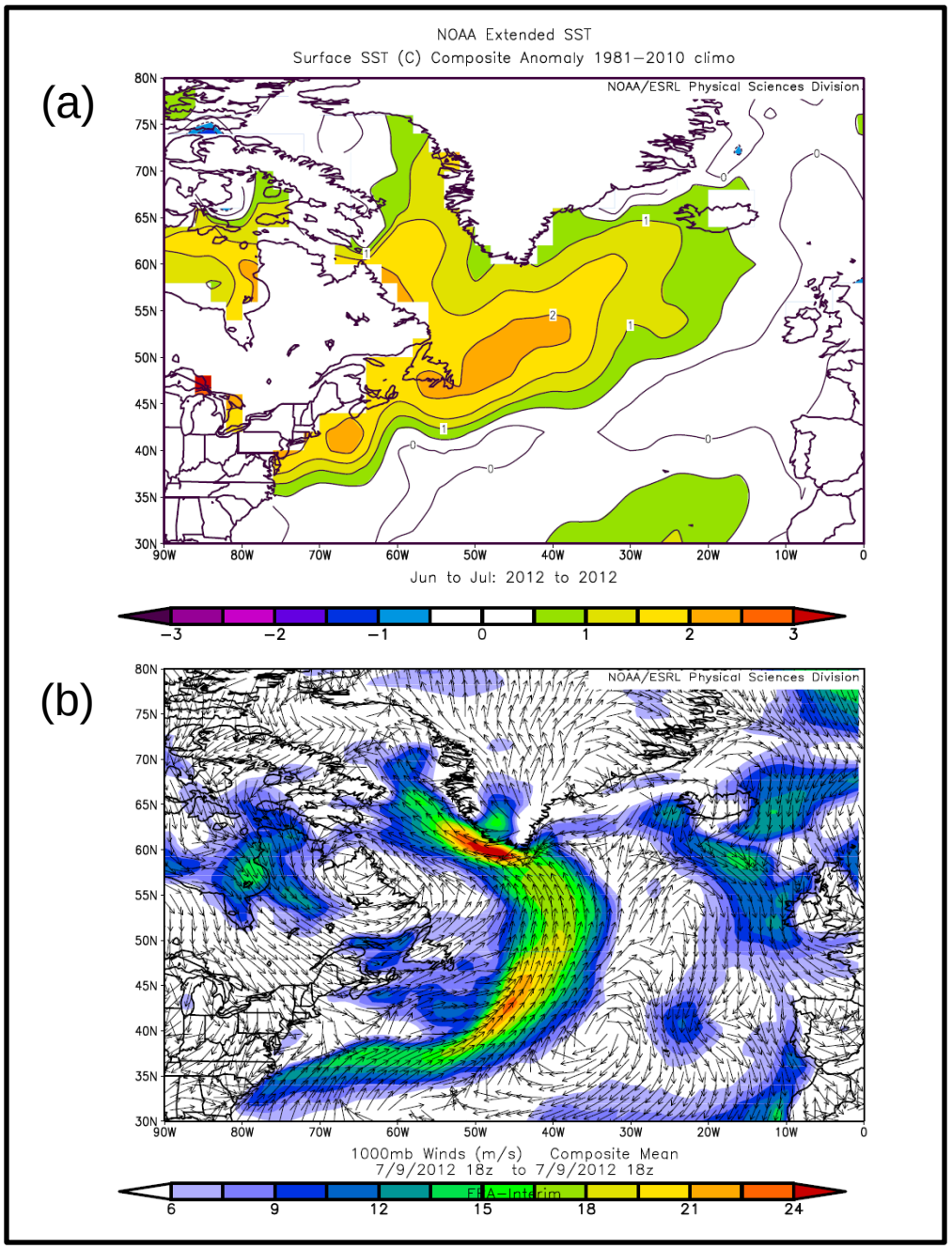

Figure S2. (a) SST anomaly for June-July 2012 (ºC) showing a positive anomaly of 2 ºC just south of Greenland and along the path of the AR described in Figure 3. (b) 1000 hPa winds for 9 July 2012 from ERA Interim Reanalysis (Dee at al. 2011), just prior to the July melt episode showing high winds near the ocean surface and along the path of high IWV air. Note that the reanalysis method interpolates winds into regions of terrain.

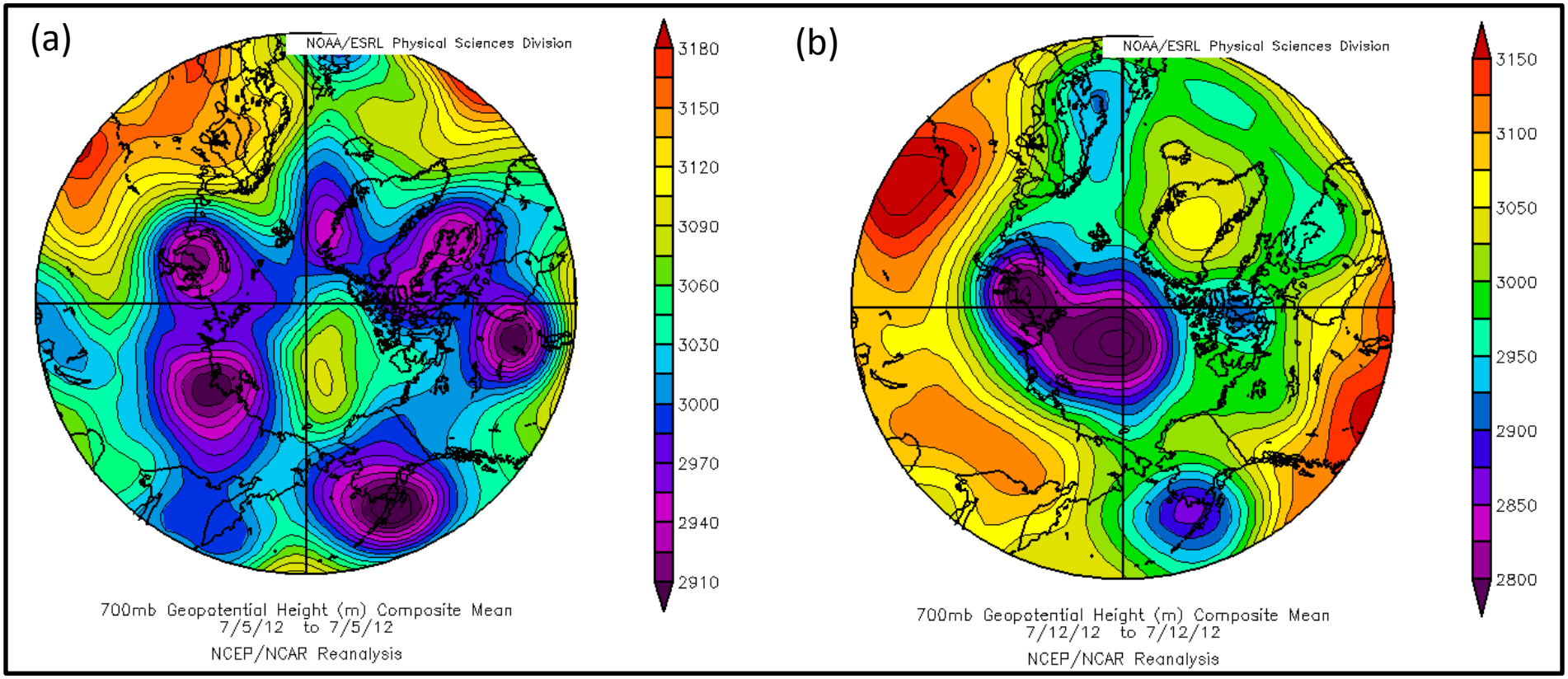

Figure S3. 700 hPa geopotential heights on the 5th (a) and 12th (b) of July 2012 showing the rapid transition from a very disturbed polar vortex (negative AO) to a simple Wave-One pattern with low pressure centered over the high Arctic (postive AO). Contour interval in (a) is 15 m and in (b) is 25 m.

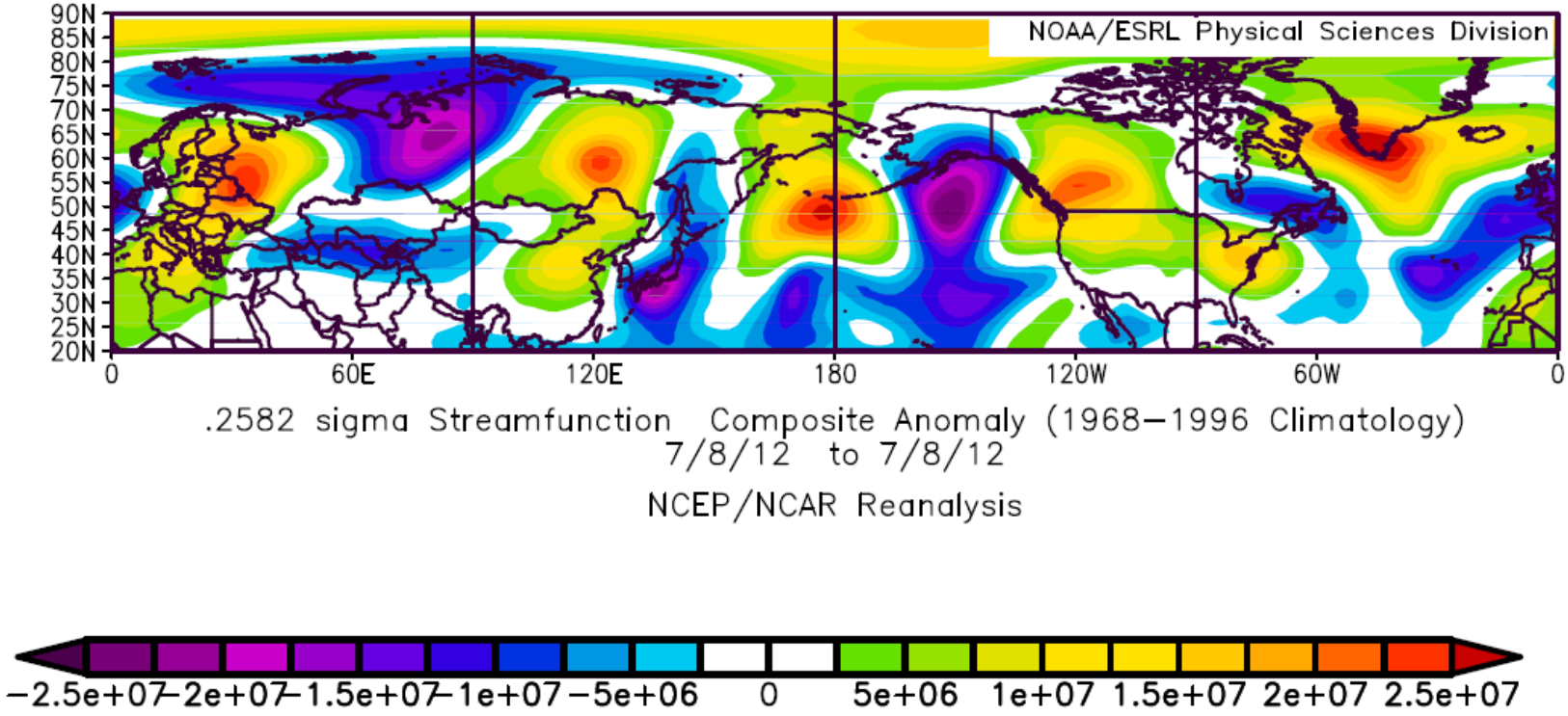

Figure S4. 0.2582-sigma level (~250 hPa) streamfunction showing five maxima very similar in locations (although a bit further north over North America and Greenland) to the first EOF identified by Teng et al., (2013).

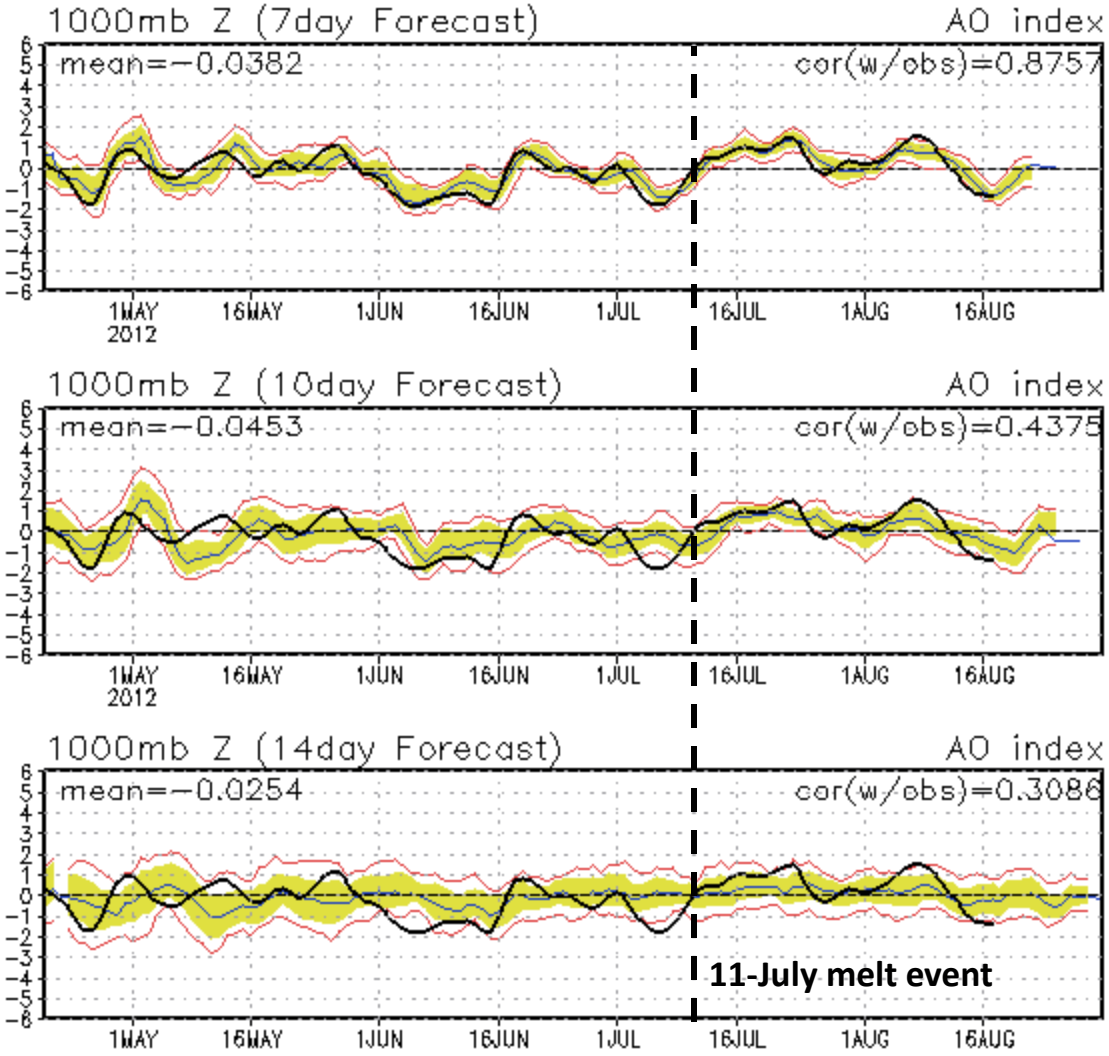

Figure S5. 7-, 10-, and 14-day GFS forecasts of the Arctic Oscillation showing reasonable skill in capturing the major negative excursion in early July at 7 days but approaching climatology at 14 days. The ensemble mean (blue curves) and spread (yellow) are shown with observations shown in black. The 11-July event is shown by the vertical dashed line. Forecast analysis downloaded from NOAA/NWS/CPC on 17 August 2012 (http://www.cpc.ncep.noaa.gov/products/precip/CWlink/daily_ao_index/ao_index_ensm.shtml)

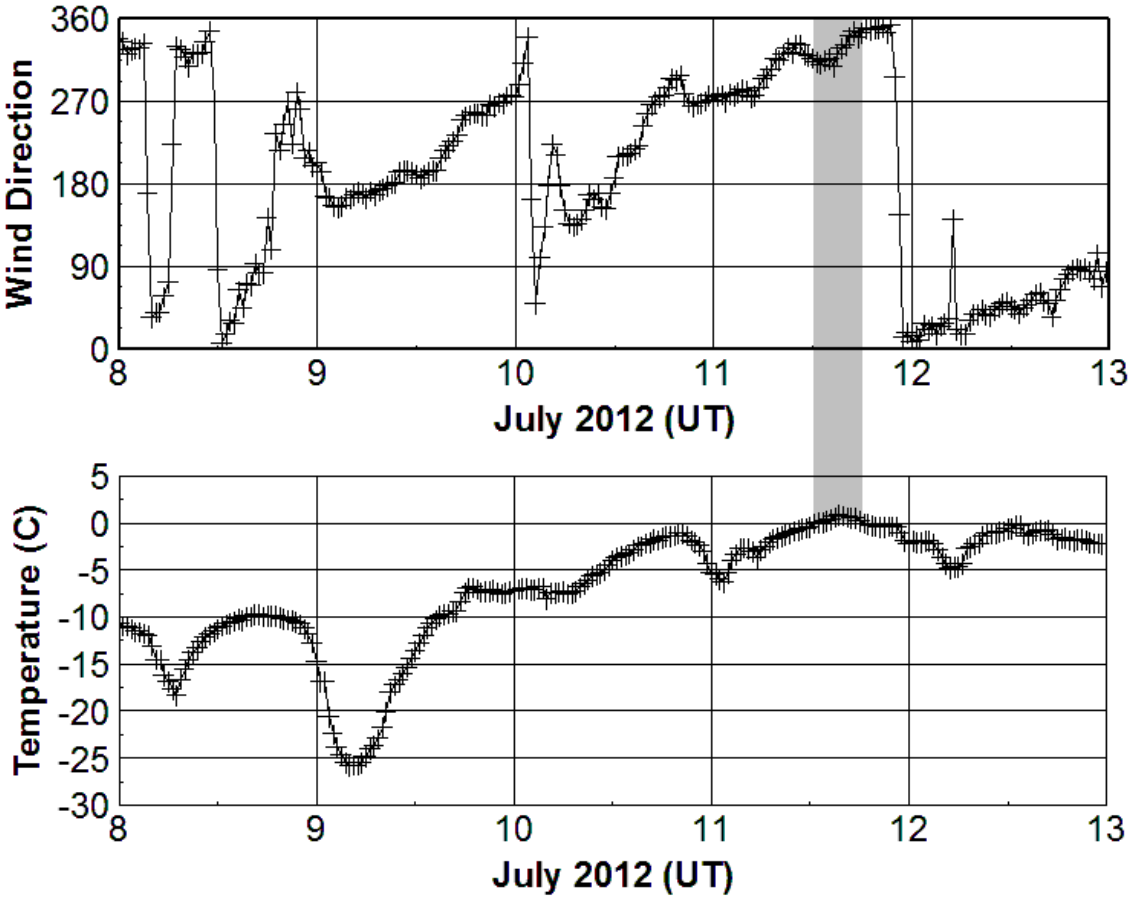

Figure S6. 10-m wind direction and 2-m temperature for Summit Station, 8-13 June, 2012. During 10 July, the temperature approached the melting point in the afternoon (local time is 3 hours less than GMT) but did not exceed it until 11 July. In both cases the winds were from the west to northwest near the surface and aloft (not shown).

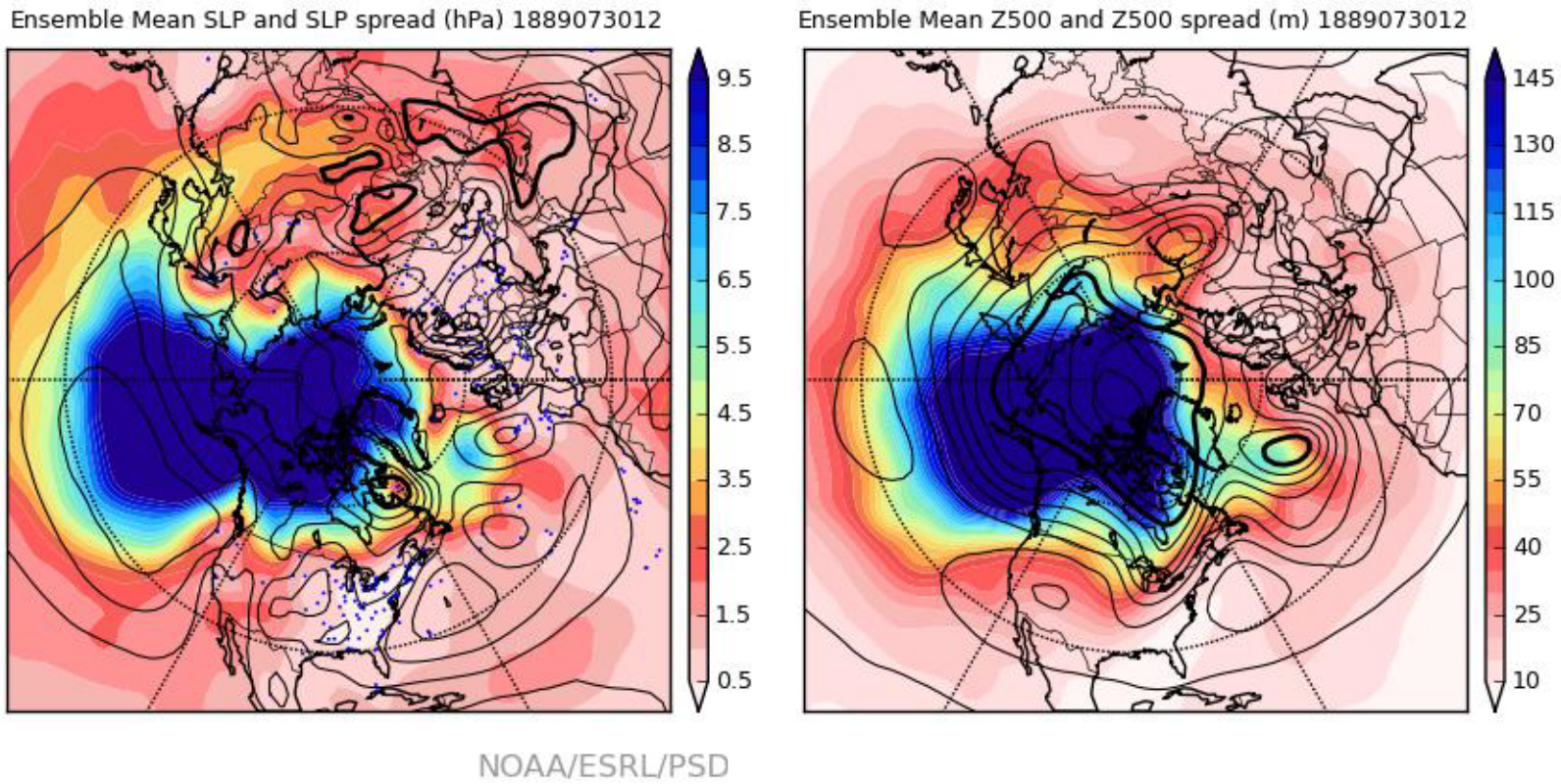

Figure S7. Ensemble mean and standard deviation (spread) for sea-level pressure (SLP) and 500 hPa heights (Z500) for 30 July 1889 showing reduced spread over mid-North America, the Labrador Sea and southern Greenland. Figure courtesy of Jeff Whitaker, NOAA/ESRL/PSD.

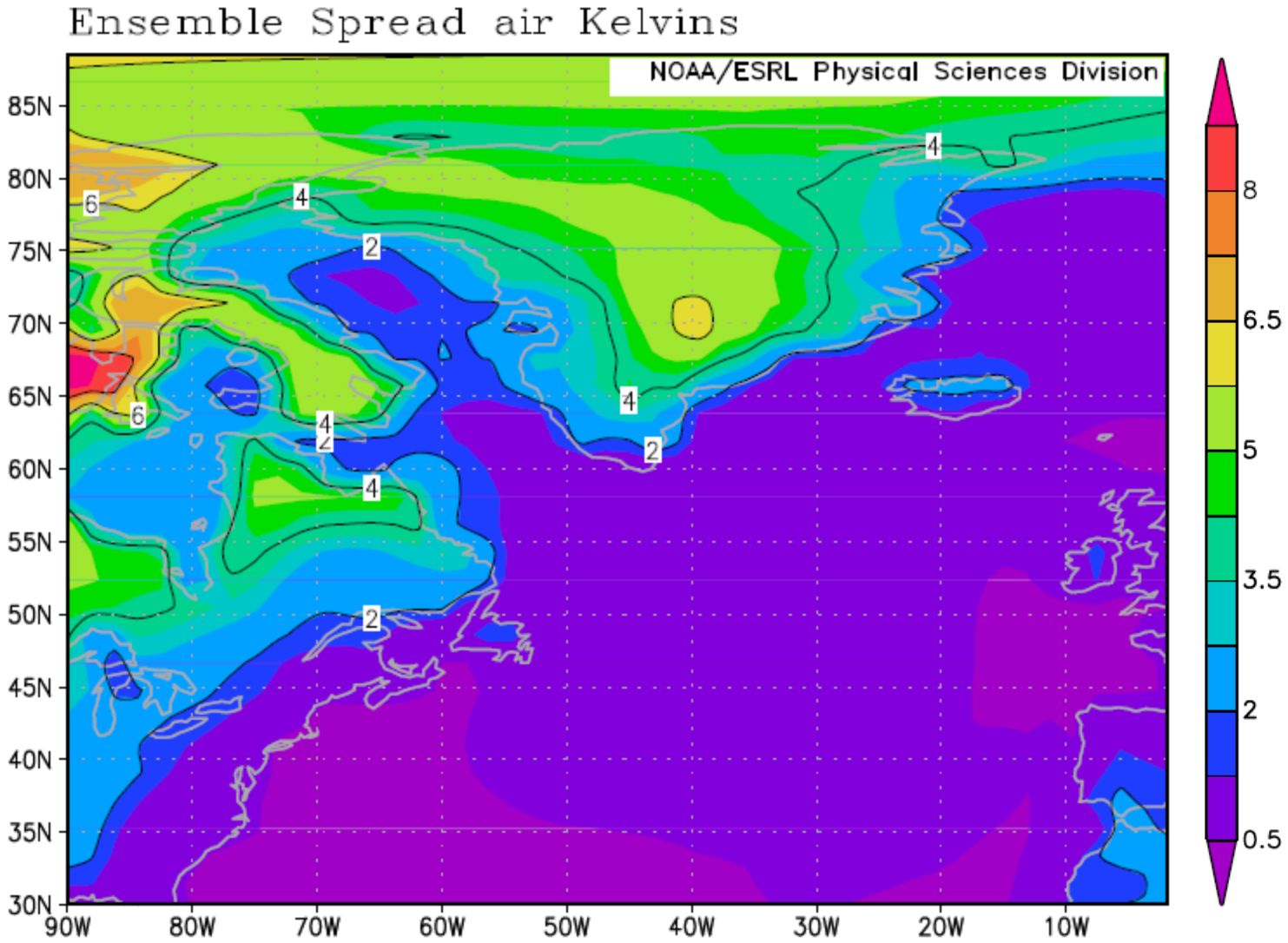

Figure S8. Ensemble standard deviation (spread) of 2-m temperature in the vicinity of Greenland for 30 July 1889. Note the spread ranges from about 2°C in coastal areas to 6°C in the vicinity of the current Summit Station. Figure courtesy of Jeff Whitaker, NOAA/ESRL/PSD.

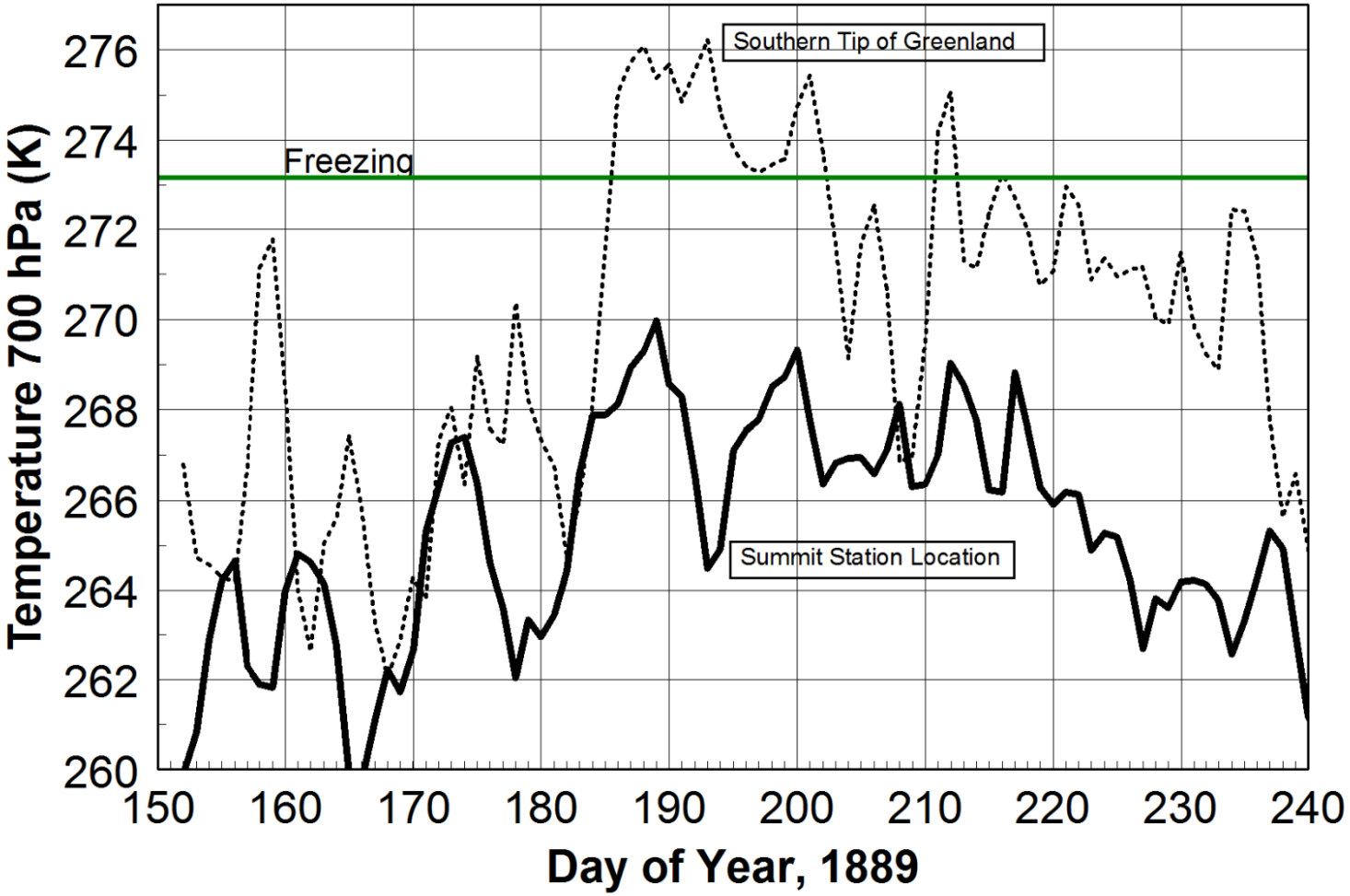

Figure S9. Time series of temperature from20CR at 700 hPa over the southern tip of Greenland and over the current location of Summit Station. The difference in absolute temperatures is within the ensemble spread of the 20CR.

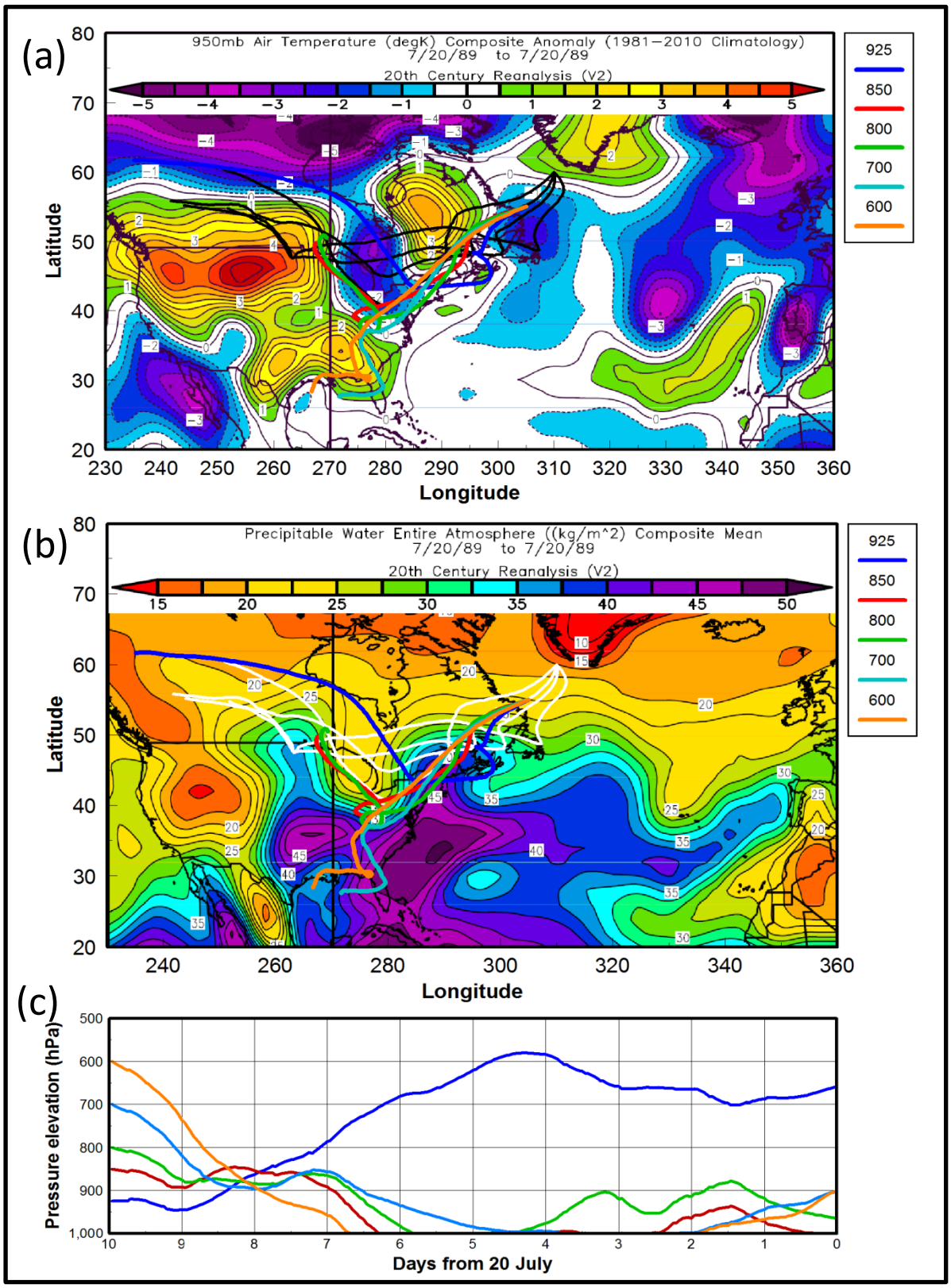

Figure S10. (a) Map of 950 hPa air temperature on 20 July 1889 with 10-day back trajectories from 30 July originating at (60N, 310W: as in Fig. 10) and at (55N, 305W: within the IWV plume in Fig. 8). (b) Map of IWV on 20 July showing extensive moisture lying along the US east coast and the southwest Atlantic. Back trajectories are the same as in (a) except for a change in color to contrast with the background. (c) Elevation of the back trajectories from 30 July showing that most originated in the boundary layer prior to 26 July.

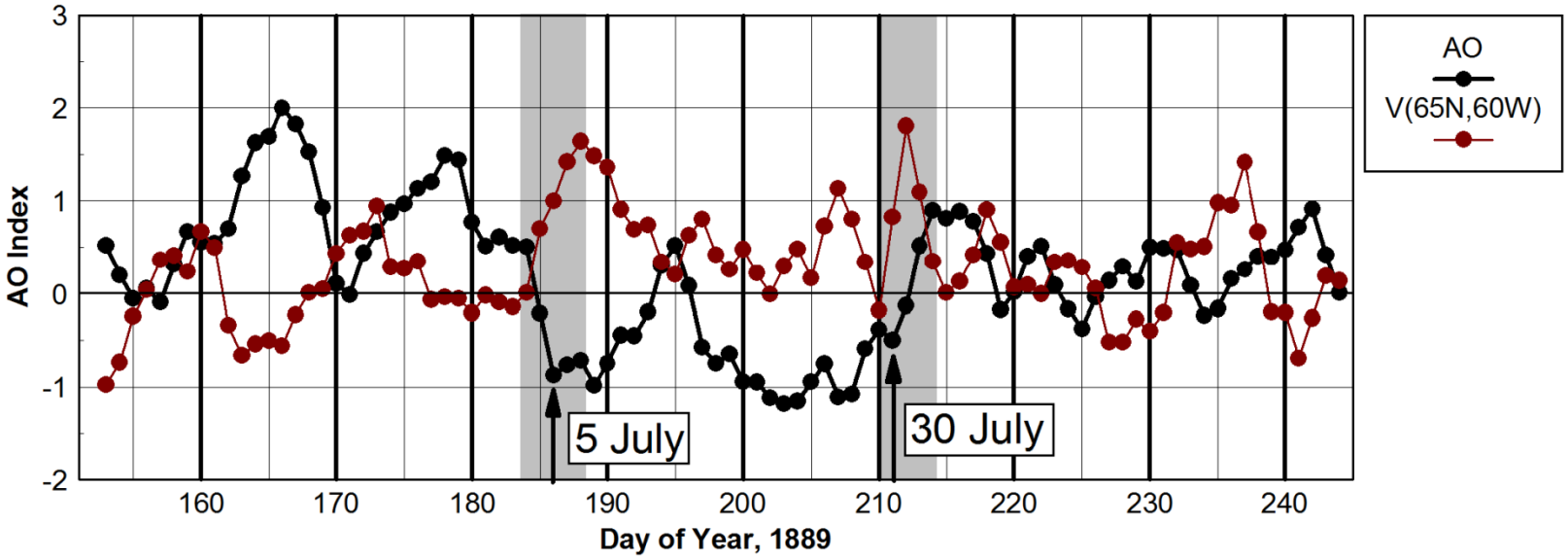

Figure S11. Time series of the Arctic Oscillation (AO) derived from the 20CR and the meridional wind speed at 800 hPa at 65N and averaged from 50W to 60W ($ms^{-1}/4.0$ for plotting purposes). Excursions in the AO and increases in V are highlighted in gray for our proposed candidate melt periods following 5 July and 30 July. The two time series are anticorrelated with $r^2=0.27$.

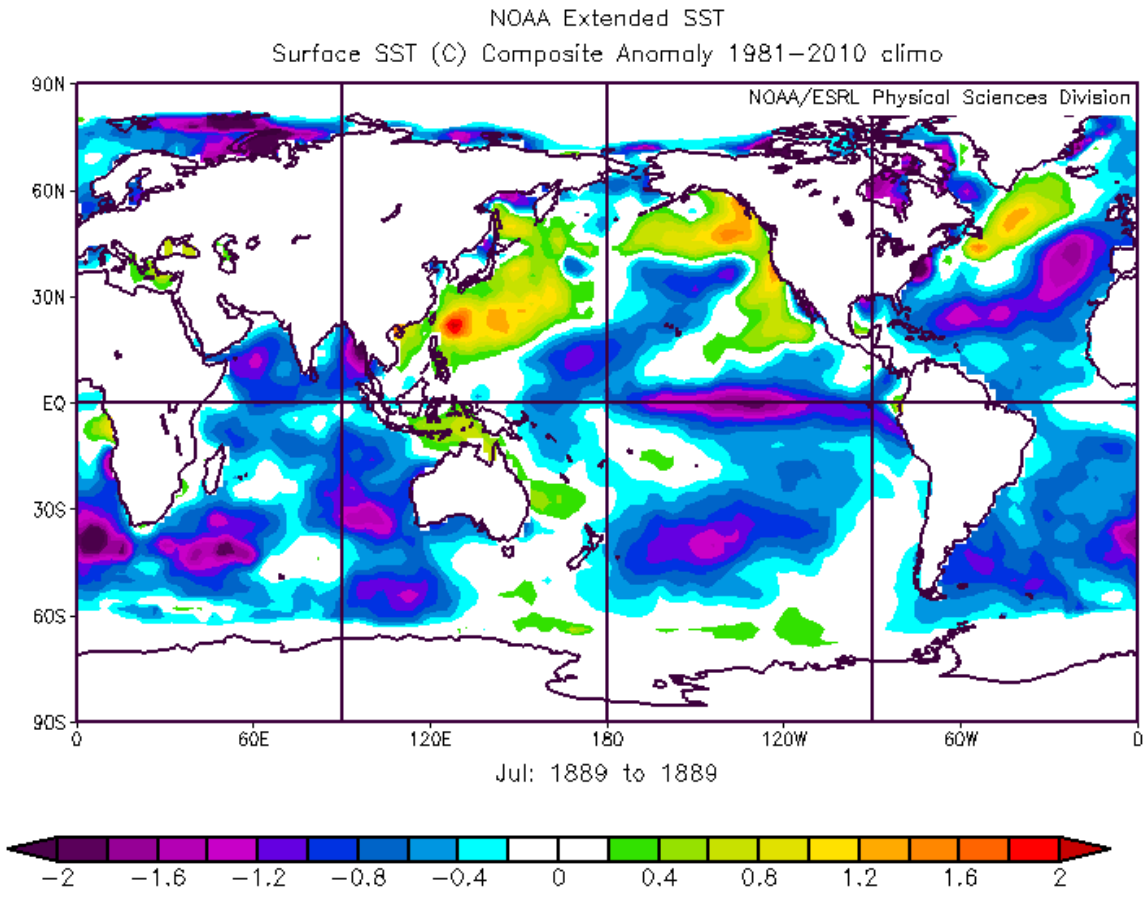

Figure S12. SST anomalies for July 1889 showing warm ocean waters just south of Greenland and the cold equatorial waters in the Pacific that are normally associated with mid-west drought in North America.

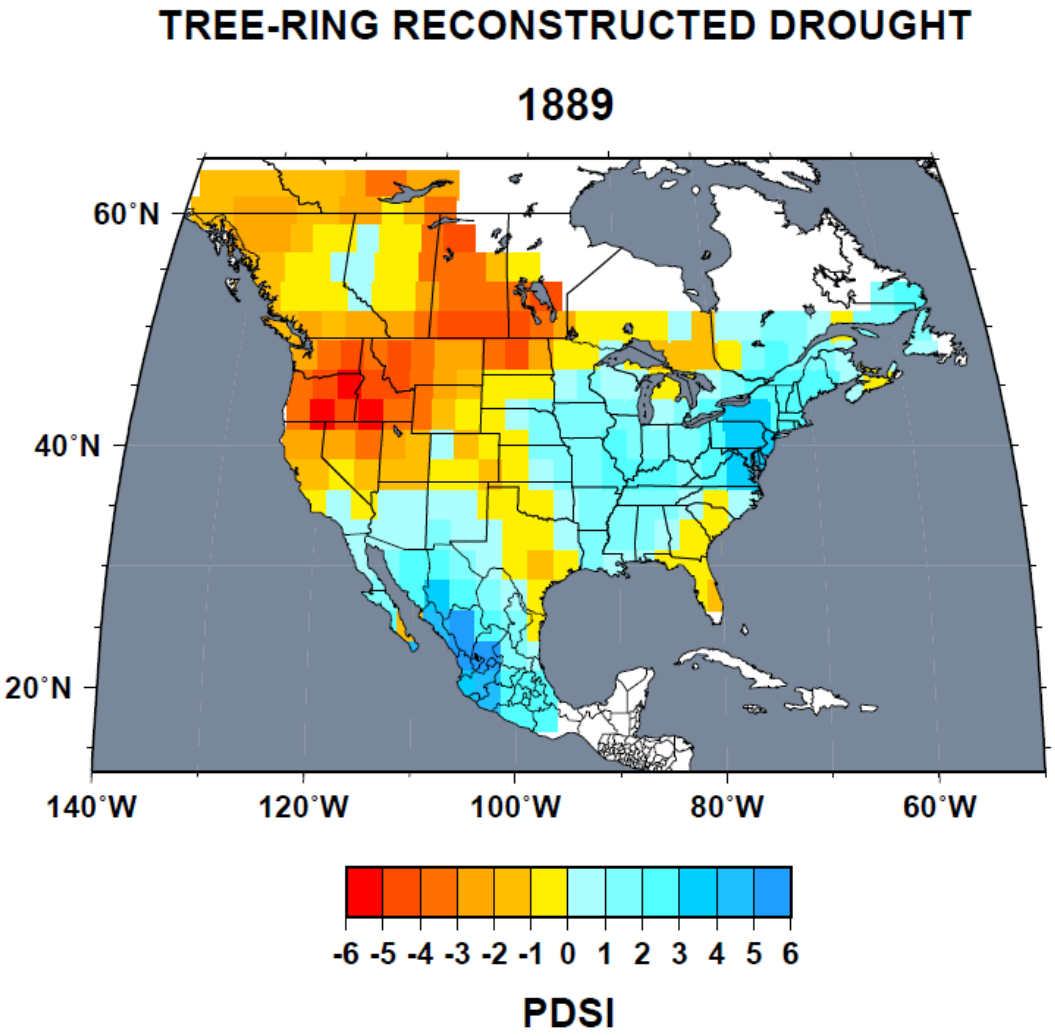

Figure S13. Tree ring reconstructed Palmer Drought Severity Index (PDSI) for 1889 from the North American Drought Atlas (http://iridl.ldeo.columbia.edu/SOURCES/.LDEO/.TRL/.NADA2004/.pdsi-atlas.html)